Quantum Electronics **50** (8) 756–762 (2020)

https://doi.org/10.1070/QEL17221

Peculiarities of the formation of photonic nanojets by a matrix of dielectric microtoroids

Yu.E. Geints, E.K. Panina, A.A. Zemlyanov

Abstract. **We report the results of theoretical modelling of photonic nanojets (PNJs) formed by laser radiation scattering on a single-layer ordered assembly of dielectric microtoroids placed on the surface of a transparent matrix (silicone film). Using the method of computational electrodynamics (FDTD), the main PNJ parameters (length, width, peak intensity) are analysed under the conditions of mutual influence of the light fields of neighbouring microparticles. It is shown that the main factor affecting the PNJ characteristics under study is the spatial configuration of the radiation-scattering particle, namely, the internal diameter of its cross section. It is found that for certain configurations of toroid placement in a cluster, a PNJ ensemble is implemented with parameters significantly better than those for a single toroid.**

Keywords: *near-field focusing, photon nanojet, microassembly of particles, microtoroid.*

1. Introduction

Currently, near-field optics is an intensively developing scientific and engineering area. The possibility of designing optical devices that combine high spatial resolution and operation speed, as well as the ability to change the frequency and power of radiation, opens up prospects for the development of new energy and resource-saving technologies. The range of scientific and applied problems related to the possibility of localisation of the electromagnetic field generated by an extended source in the region of nanometre dimensions is also constantly expanding [1, 2].

According to classical concepts, the spatial resolution of optical devices is limited by diffraction, and the minimum size of the focal spot cannot be less than half the wavelength of light ($\lambda/2$) in the medium. However, this statement implies that the optical circuit elements are located at a considerable (compared to λ) distance from each other. At the same time, numerous studies have proved the appearance of a region of high-intensity optical field localised in space when the wave is scattered on a weakly absorbing dielectric particle (Mie scattering). This effect is referred to in the scientific literature as the "photonic nanojet (PNJ) effect" [3–7] and is a consequence of aberrational focusing of radiation by weakly absorbing micro-objects whose characteristic size R is close to the wavelength of incident radiation (mesoscale particles, $R \approx \lambda$). In contrast to the case of focusing radiation with a conventional optical lens, the PNJ specificity is that it is formed in the near-scattering zone, where the optical field is characterised by the most complex spatial structure defined by a superposition of outgoing and decaying (evanescent) waves [8, 9]. This allows for a more significant localisation of the optical field in the near-field focusing region than in the far diffraction zone. In particular, when irradiating a homogeneous microsphere in the air with a plane light wave, a spatial resolution of $\sim\lambda/3$ can be achieved, which is noticeably lower than the classical diffraction limit.

Spatial and amplitude characteristics of PNJs depend on the geometric shape of the object that scatters radiation, its optical properties, and the incident radiation wavelength [10–12]. When solving particular practical problems, varying these parameters allows one to optimise the main characteristics of the jet (length, width, and peak intensity). These include, for example, the detection of small inhomogeneities in the near-surface layer of the sample, their spectroscopic analysis, and modification of the surface relief by optical methods (formation of artificial through-channels or perforation) [13, 14]. At present, it is premature to talk about the mass introduction of the PNJ-based nanooptics devices, but it is obvious that progress in this direction will provide a breakthrough in the development of many priority areas of science and technology. The current state of research and practical applications of the PNJ effect from microparticles are presented in detail in [15–18].

Another promising area of PNJ application is surface nanostructuring using a matrix of ordered dielectric mesoscale particles [19]. It was found that individual particles combined in a cluster begin to affect neighbouring particles due to interference of optical fields. These collective effects of light scattering can significantly influence the parameters of individual PNJs.

The development of methods for obtaining ordered ensembles of micro- and nanoparticles, as well as the formation of nanostructured micro-assemblies with specified characteristics on their basis is one of the urgent problems of fundamental and applied nanooptics. To date, various methods of obtaining a micro-assembly of particles are known. Mesoscale particles can be formed on a substrate, for example, using electron beam lithography or photolithography [20]. A monolayer of densely packed spherical dielectric particles can also be deposited onto the surface when the colloidal solution dries [21, 22]. In this case, by varying the thickness of the original solution layer and its evaporation time, self-organising layers of dielectric microspheres with different characteristics can be obtained [23].

Yu.E. Geints, E.K. Panina, A.A. Zemlyanov Zuev Institute of Atmospheric Optics, Siberian Branch, Russian Academy of Sciences, pl. Akad. Zueva 1, 634055 Tomsk, Russia; e-mail: ygeints@iao.ru

Received 11 December 2019; revision received 13 January 2020
Kvantovaya Elektronika **50** (8) 756–762 (2020)
Translated by M.A. Monastyrskiy

As a rule, micro-assemblies of particles are placed on a dielectric substrate, which can be a polymer (silicone) film. The use of a silicone substrate makes it possible to fix microparticles embedded in them in various spatial configurations, and not only in the form of densely packed particles [24, 25]. Subsequently, such flexible polymer matrices can be transferred to the target surface and irradiated with a laser, which will lead to a multiple increase in the optical field intensity in the PNJ focus regions.

The PNJ characteristics were previously studied in detail in [26–28] for scattering laser radiation by a single-layer ordered assembly of dielectric microparticles of various spatial shapes (sphere, axicon) embedded into a transparent matrix (silicone film). It is shown that certain spatial configurations of micro-assemblies allow forming a PNJ ensemble with specific characteristics unattainable for isolated (single) microparticles. In addition, ordered particle clusters have an advantage in terms of comprehensive assessment of jet parameters.

One of the problems of near-field focusing is the small spatial extent of the focal region formed near particles of classical convex geometry (sphere, cube, cylinder, pyramid, and cone), which usually does not exceed several radiation wavelengths [8, 11]. This stimulated the search for microparticles of other geometric shapes that would make it possible to increase the PNJ length and remove it as far as possible from the microlens surface.

In recent work by Zhang et al. [29], PNJs formed by dielectric circular microtoroids were theoretically studied. Cases of PNJ generation from single particles in air, water, or on a dielectric substrate were considered. It was found that single toroids with a refractive index $n = 1.5$ in air can generate ultralong PNJs (up to 67.36λ in length). Increasing the refractive index of toroids reduces the PNJ length. For example, particles with $n = 3.5$ form PNJs with a length of $\sim$3.66λ. It was also noted that changing the geometric parameters of a microtoroid allows for variation of the PNJ characteristics (length, width, and peak intensity).

It should be noted, however, that Zhang et al. [29] determined the total PNJ length using the formula $L = L_f + L_d$, where L_f is the focal length, i. e. the distance from the particle surface to the region with a maximum intensity B_{max} in the longitudinal field distribution, and L_d is the distance from the region where the field intensity is equal to B_{max} to the point at which the intensity decreases by e^2 times. The choice of such a criterion for estimating the PNJ length gives admittedly higher L values than when determining the PNJ length by the FWHM level [26, 27].

In practice, not single microparticles are more in demand, but their assemblies located on a transparent substrate. Collective interference effects arising from the interaction of fields scattered by particles with the substrate remained outside the scope of work [29].

In this work, we present the results of numerical simulation of near-field focusing of a light wave by a single microtoroid, as well as an array of microtoroids placed on a transparent silicone matrix at the nodes of a rectangular spatial lattice. It is shown that the presence of neighbouring particles can radically change the characteristics of the generated PNJs due to the manifestation of destructive interference of fields. At the same time, by fine-tuning the placement period and geometric parameters of the microtoroids themselves, it is possible to reduce the impact of collective effects and change the parameters of light nanojets formed in order to increase their intensity and length.

2. Numerical simulation technique

As a basic particle, we consider an open dielectric microtoroid in the form of a ring formed by the rotation of a circle with a radius of R_2 around the axis parallel to one of its diameters and not intersecting it (Fig. 1a). The distance between the toroid centre and the centre of its circular section is denoted by R_1, and the radius of the toroid's inner hole is denoted by R_3. In this case, the toroid's outer radius is $R = R_1 + R_2$. Cases were considered when either a single toroidal particle made of nonabsorbing glass with a refractive index $n = 1.6$, or an array of identical microtoroids separated by a distance g, were located on a silicone substrate being a nonabsorbing organic polymer film with a refractive index 1.44 in the visible wavelength range (Fig. 1b). It was assumed that the microparticles were located in the air ($n_0 = 1$).

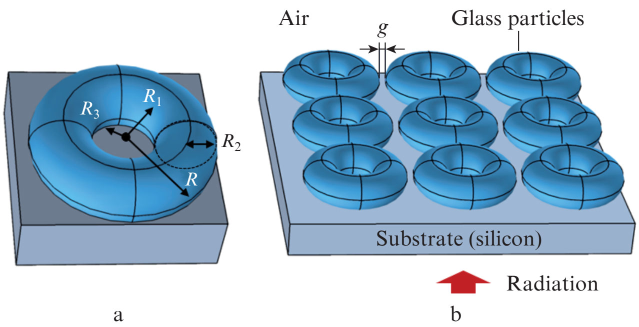

Figure 1. Schematic of (a) a single toroid and (b) a microassembly of glass toroids located on a silicone substrate.

The numerical calculation of the near-field structure in diffraction of a light wave by a single particle, as well as an assembly of identical microparticles, was performed by computational electrodynamics technique (FDTD) using the Lumerical FDTD Solutions commercial software package. In fact, a system of Maxwell's of differential equations was solved for the electromagnetic field in four-dimensional space. The numerical simulation technique was similar to that previously employed in [26]. The numerical solution accuracy was controlled by an adaptive computational grid, whose nodes were condensed in the regions of sharp gradients of the medium's permittivity (particle boundaries). The total number of grid nodes was several tens of millions with spatial and temporal steps of the computational scheme of about 2 nm and 0.06 fs, respectively. Note that due to the spatial symmetry of the microassembly itself, the ensemble of closely spaced particles was only simulated for a single microtoroid on the substrate. In this case, the periodicity conditions for scattered fields in the form of Floquet–Bloch relations [30] were set at the computational domain's boundaries being parallel to the direction of optical radiation propagation, while at other boundaries (perpendicular to the light incidence), so-called perfectly matched layers (PMLs) were constructed for the fields in order to reduce the parasitic effects in wave reflection.

A linearly polarised monochromatic optical wave with λ = 0.532 μm propagated through the microparticle assemblies in the positive direction of the z axis and formed a diffraction pattern in the near scattering field $\boldsymbol{E}(x, y, z; t)$. For further analysis, this spatiotemporal distribution was averaged over an interval of two picoseconds, which was estimated to be sufficient to account for all the transient processes occurring in micrometre particles and in the substrate. The relative electric field intensity of the optical wave $B(x,y,z) = |\boldsymbol{E}(x,y,z)|^2/E_0^2$ (E_0 is the incident wave field amplitude) in the vicinity of each microtoroid was studied. The dimensional and amplitude characteristics of localised regions of increased intensity (PNJs) formed near the centre of particles were determined.

3. Simulation results

First of all, let us consider the peculiarities of the PNJ formation from an isolated (single) toroid located on a silicone substrate. Basically, we will be interested in the effect of the inner aperture radius R_3 of a nonabsorbing glass toroid on the characteristics of the PNJs formed by it. This parameter is important because it determines the optical activity of the particle.

The corresponding two-dimensional tonal distributions of the relative intensity of the optical field $B(x,z)$ are shown in Figs 2a–2c, and the longitudinal profiles of the field intensity in the PNJ region are shown in Figs 2d–2f. For definiteness, the inner cross-section radius R_3 of the toroid was selected equal to $0.3R$, $0.5R$ and $0.7R$. Radiation falls from left to right. It should be noted that due to the requirement to preserve the outer size $R = 2\lambda$ of the toroid and the circular shape of its cross section, changing the internal diameter of the toroid entails a change in its cross-section radius: $R_2 = R - R_3$.

It is seen that the incident radiation is scattered in a certain way by the toroid surface, forming an ordered localised structure along the z axis. The superposition of all circular sections of the toroid forms a complete picture of the field with allowance for the hole inside the particle. As follows from Fig. 2d–2f, the longitudinal profile of the field is formed by several sections in which the intensity increases and decreases due to interference of interacting fields. The maximum intensity and length of these sections are different, which introduces certain difficulties in estimating the photon flux length.

To quantitatively estimate the PNJ parameters, we will determine the PNJ width along the two coordinate axes R_{jx}, R_{jy} and the PNJ spatial length L at the level of the field intensity FWHM. For the PNJ length, we take the length of the 'operating' zone corresponding to the principal maximum in the longitudinal distribution of the optical field along the z

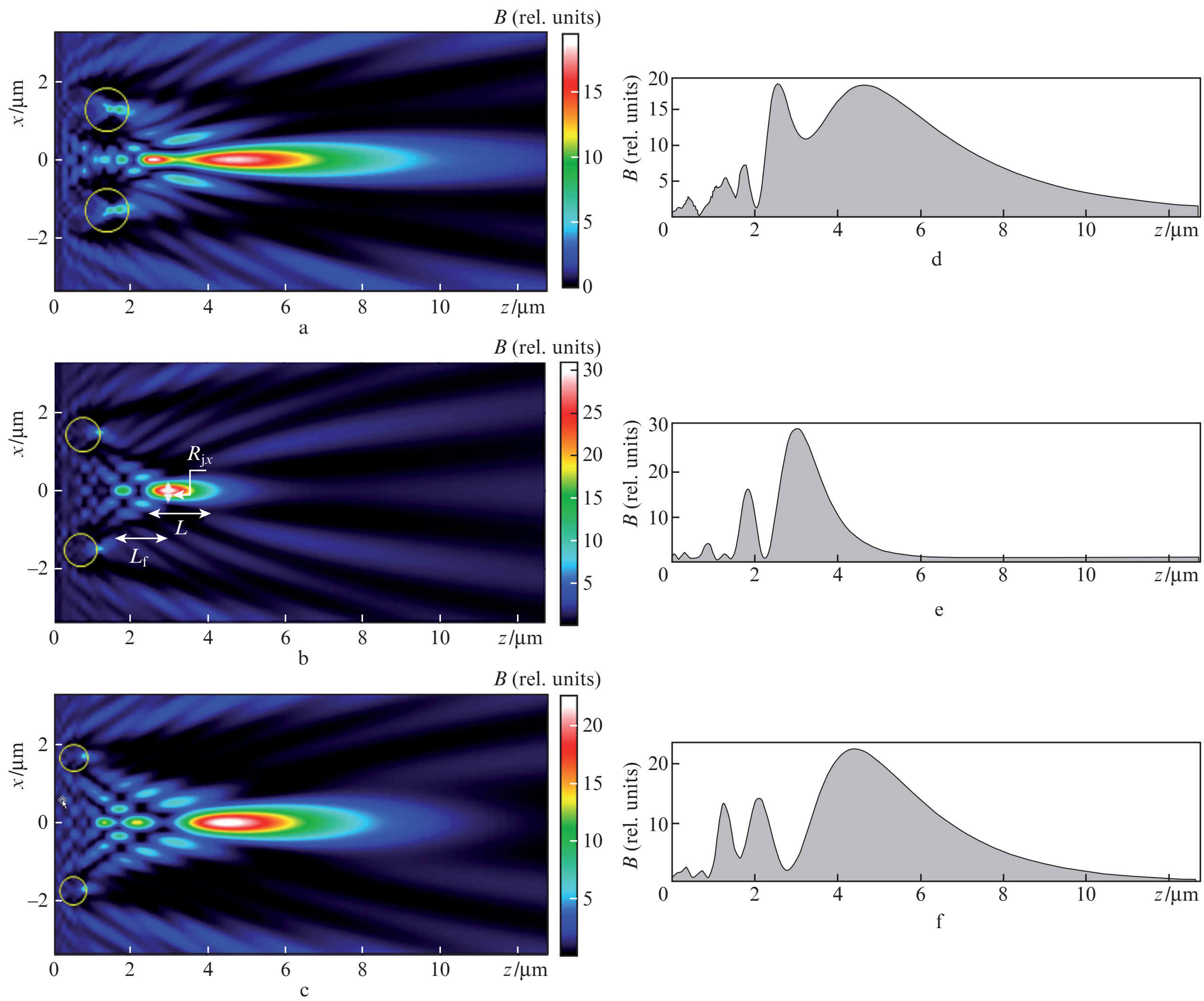

Figure 2. (Colour online) (a, b, c) Two-dimensional and (d, e, f) radial distributions of the relative optical field intensity $B(x,z)$ in the vicinity of glass toroids with a radius $R = 2\lambda$ and various internal structures, illuminated by radiation with $\lambda = 0.532$ μm. The inner hole radius of the toroid is $R_3 =$ (a, d) $0.3R$, (b, e) $0.5R$, and (c, f) $0.7R$.

axis. We will also make allowance for the parameter L_f, the focal length defined as the distance from the particles' surface to the principal intensity maximum (see Fig. 2b). The PNJ amplitude characteristic is the peak (relative) intensity B_m of the optical field in the near scattering zone. For a comprehensive assessment of the degree of PNJ spatial localisation, we also use the PNJ quality criterion $Q = B_m L/\min\{R_{jx}, R_{jy}\}$ [31].

Numerical estimates of these parameters are shown in Fig. 3. For comparison, it also presents the corresponding values of length L_s, width along the two coordinate axes R_{sx} and R_{sy}, peak intensity B_{sm}, and quality parameter Q_s for a spherical particle with a radius $R = 2\lambda$ and a refractive index $n = 1.6$.

Figure 3 shows that the PNJ characteristics under study are very sensitive to changes in the toroid configuration. In particular, microtoroids with a relatively small ($R_3 \approx 0.3R$) or, conversely, a large ($R_3 \approx 0.7R$) inner hole radius lead to fairly extended jets with $L \approx 10\lambda$. However, if in the first case the PNJ intensity maximum is located near the particle surface, then in the second case it is removed by a distance of $L_f = 7\lambda$. This effect is accompanied by a broadening of the PNJ transverse size and, as a result, a decrease in the peak intensity B_m.

Particles with the inner hole radius $R_3 \approx (0.5-0.6)R$ form PNJs with the most stable spatial parameters. The intensity maximum is located outside the particle's surface in the PNJ zone characterised by a sub-diffractive transverse size and a sufficiently large amplitude ($B_m \approx 30$). It should be noted, however, that of all the options discussed above, this microtoroid configuration implements the minimal PNJ length ($L \approx (1.5-3)\lambda$). Also, noteworthy is an abnormal decrease in the B_m intensity at $R_3 \approx 0.9R$. Obviously, such an ultrathin ring cannot be considered as a promising object for sub-diffraction localisation of the optical field.

The numerical estimates given above show that a peculiarity of the field formation in the near-field scattering region is, as a rule, the dominance of only one key PNJ parameter. By choosing an appropriate configuration of microparticles, we can significantly improve the PNJ characteristics, in particular, increase the intensity and length, and reduce the transverse size to sub-diffraction values. This circumstance is extremely important when choosing, for example, a particular experimental 'particle + radiation' configuration for obtaining PNJs with specified properties, since different practical tasks require the creation of different types of photon fluxes with specific characteristics. For example, when using microparticles for contact perforation of cell membranes, the maximum-intensity PNJs are required, and their length does not play a significant role, while for nano-sensorics and optical surgery, the narrowest and most elongated light jet is required.

In general, comparing the parameters of the PNJs formed by a single toroid and a sphere, it should be noted that regardless of the inner hole diameter, a nonabsorbing glass toroid always forms jets of a greater length than a sphere with similar optical properties. The undoubted advantage of spherical microparticles is their ability to focus the optical field into spatially localised regions with ultrahigh intensity. At an ext-

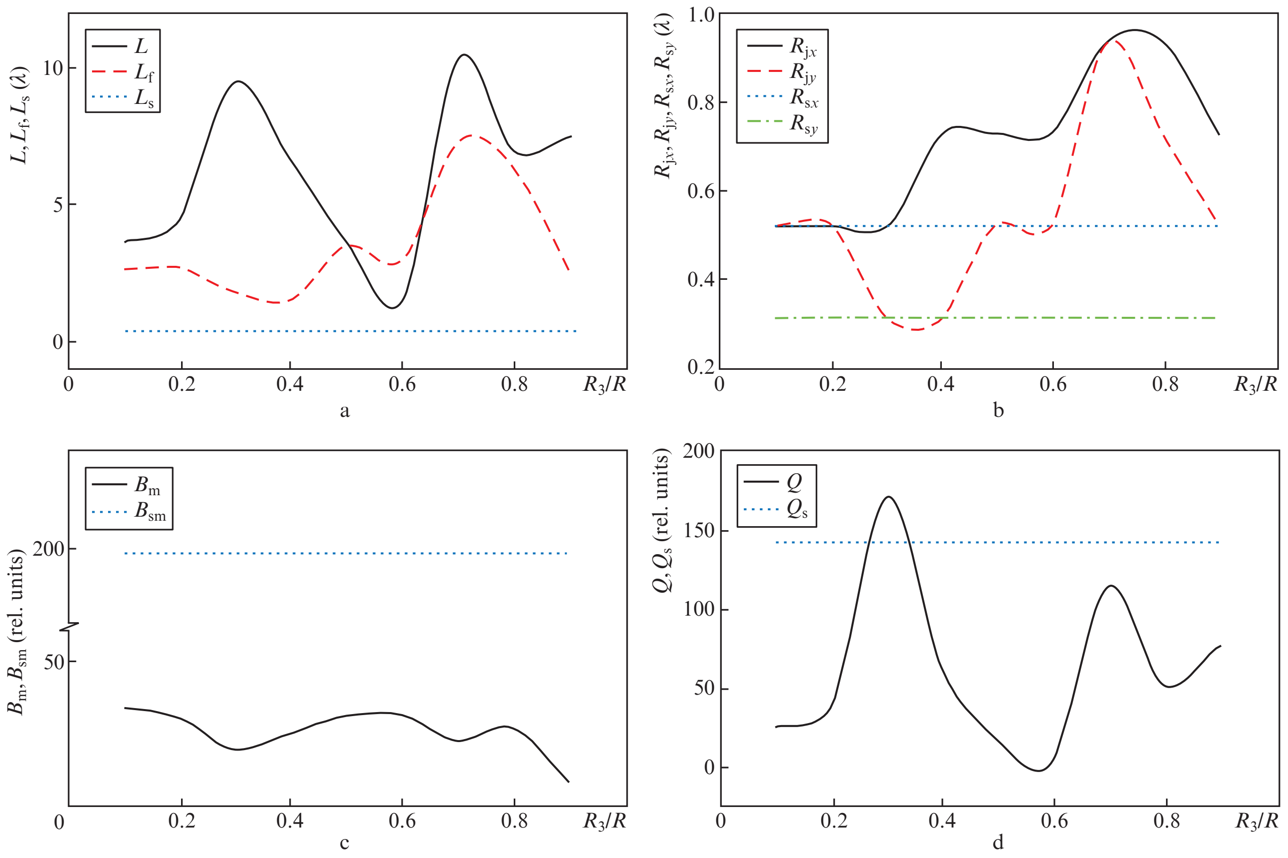

Figure 3. Parameters of the PNJ formed by a single toroidal particle located on a silicon substrate when varying its inner hole radius R_3: (a) length L and focal distance L_f, (b) transverse size $R_{j(s)}$, (c) peak intensity B_m, and (d) quality parameter Q. Dashed lines correspond to the PNJ parameters for a spherical particle.

remely short jet length ($L \approx 0.37\lambda$), its intensity reaches peak values $B_m \approx 200$, which is several times higher than the corresponding value for the toroid.

Numerical estimates of the PNJ complex quality parameter Q, obtained from calculations of the PNJ dimensional and power characteristics with allowance for the structural composition of glass microtoroids are presented in Fig. 3d. We have found that for the inner hole radius of the toroid $R_3 \approx (0.25-0.35)R$ it becomes possible to implement a photon flux with a quality parameter significantly higher than that for a spherical particle.

Next, we have to look at how the parameters of the formed PNJs change when a single particle is replaced by a cluster of identical microparticles located on a transparent substrate. The distance between individual particles is regulated by the parameter g which is measured in units of the total radii R of the toroid. We have considered situations where the distance between particles in the cluster is varied from $g/R = 0$ to $g/R = 1$, which corresponds to different types of toroid packing, i.e. from dense to sparse, respectively.

As an example, Fig. 4 shows the tonal distributions of the relative intensity $B(x,z)$ of the optical field for a single-layer cluster of densely packed particles ($g = 0$). As in the case shown in Fig. 2, the inner hole radius of the toroid is $R_3 = 0.3R$, $0.5R$, and $0.7R$.

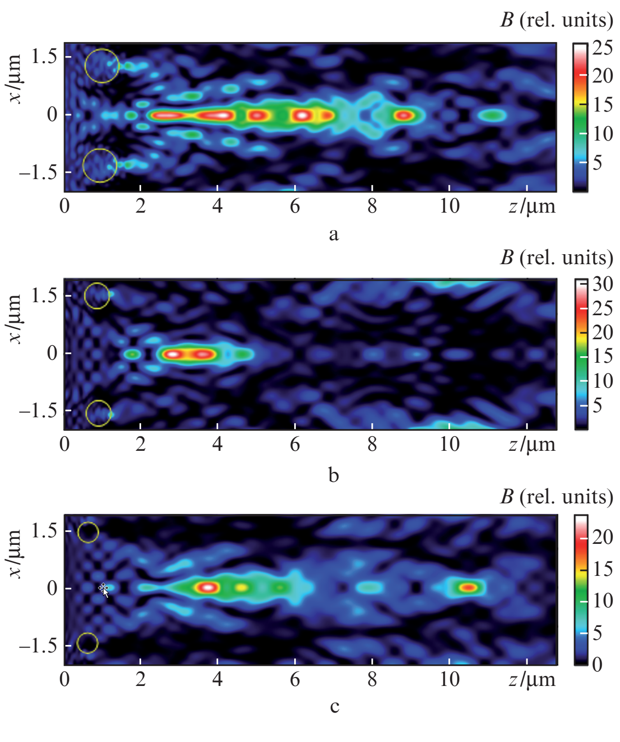

Figure 4. (Colour online) Two-dimensional distribution of the relative optical field intensity $B(x,z)$ in the vicinity of a cluster of densely packed glass toroids ($g = 0$) with a radius $R = 2\lambda$ and various internal structures. The inner hole radius of the toroid is R_3 = (a) $0.3R$, (b) $0.5R$, and (c) $0.7R$.

It is obvious that for densely packed particles, the longitudinal PNJ structure becomes more complex and reflects the influence of collective interference effects on the photon flux transformation. It can be seen that, in addition to the principal intensity maximum in the radial direction, secondary field maxima appear, which, although they have a lower intensity than the principal PNJ, are quite localised in the transverse direction and elongated along the light flux direction. The total length of such intermittent PNJ increases significantly, which may become a fundamental point in the implementation of certain practical applications. It should also be noted the appearance of clearly defined side lobes directed at an angle to the principal optical flux in the near-field distribution for toroids with a large inner hole size (Fig. 4c).

Increasing the distance between toroids (sparse packing of particles) leads to a weakening of the impact of neighbouring particles and, as a result, to a smoothing of the PNJ longitudinal profile. At $g/R > 1$, the characteristics of PNJs formed by a single-layer array of glass toroids become close to those for an isolated particle. This fact is illustrated in Fig. 5, which shows the results of numerical calculations of the key PNJ parameters, namely, its length L and the maximum relative intensity of the optical field B_m for various particle packing in the cluster.

Since, as shown above, the PNJ longitudinal profile is characterised by significant inhomogeneity, we separately determine the principal peak's extent L_b with the maximum intensity B_m, as well as the total jet length L, taking into account all the secondary field bunches. We should recall that the PNJ width R_j and spatial length L are determined at the FWHM level of the field intensity. For definiteness, the inner radius R_3 of the toroid is chosen equal to $0.5R$. For comparison, the PNJ lengths and intensities for a single microtoroid are shown in Fig. 5.

It follows from Fig. 5a that the immediate environment of each toroid significantly affects the length of photon fluxes formed in the near-field scattering zone. The greatest variability of this parameter is observed for a densely packed matrix of particles ($g/R \approx 0-0.5$). However, starting from $g/R \approx 0.6$, the jet length stabilises at a certain level and no longer depends on the location of particles in the cluster. For comparison, the length of the principal intensity maximum of the PNJ formed by an isolated particle located on a silicon substrate is $L_b \approx$ 1.25 mm (dashed line in Fig. 5a). In this case, the total PNJ length, with allowance for all secondary field maxima, is $L =$ 2.5 μm. It should also be noted that for the selected configuration of toroids ($R_3 = 0.5R$, $R = 2\lambda$) the transverse size of the jet varies slightly and corresponds to the classical diffraction limit $R_{jy(jx)} = 0.52\lambda \approx \lambda/2$.

Figure 5b shows the results of numerical calculations of another important PNJ parameter, namely the maximum relative optical field intensity B_m. Due to interference of the fields of neighbouring jets, a denser packing of toroids inevitably leads to pulsations of their intensity and may cause a spatial 'break' of an initially continuous PNJ into separate segments along the path of the optical wave propagation (see Fig. 4). As the distance between the particles increases, the impact of collective interference effects weakens, which leads to a smoothing of the $B_m(g)$ dependence. Nevertheless, it should be noted that a cluster of microtoroids gives consistently higher B_m values than an isolated particle (dashed line in Fig. 5b), with the exception of only some variants of packing the microassembly. Consequently, the use of an array of particles in certain cases may be more attractive for the implementation of practical applications related, for example, to the processing of materials and surface perforation, where the role of this parameter is decisive.

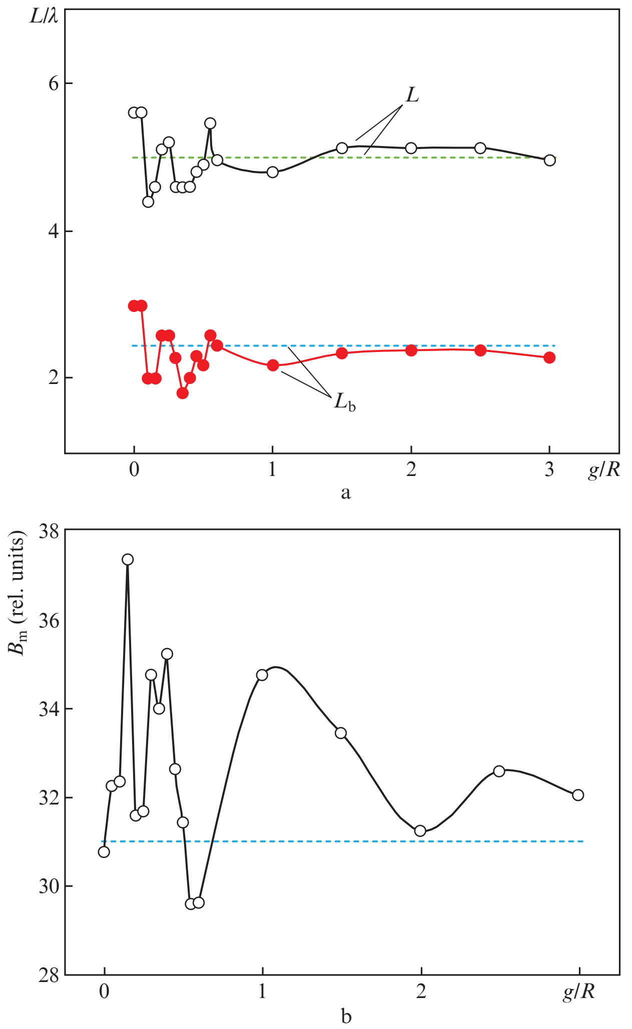

Figure 5. (a) PNJ length L and (b) peak intensity B_m for a cluster of microtoroids when varying the distance g/R between particles. Dashed lines correspond to the parameters for a single microtoroid.

4. Conclusions

On the basis of numerical simulation, we have studied the peculiarities of forming the spatial structure of the near-field scattering of a light wave on a single dielectric nonabsorbing microtoroid located on a polymer substrate, as well as on an ordered cluster of microtoroids. The PNJ characteristics as regions with a high concentration of the optical field are investigated in detail.

It is shown that the spatial shape of the radiation-scattering particle affects the main PNJ parameters, i.e. length, width, and maximum intensity. It was found that toroids with an inner cross-section radius of $R_3 \approx (0.5-0.6)R$ result in spatially localised, high-intensity light fluxes. An increase or decrease in R_3 leads to instability of the parameters under study, for example, to a sharp increase in the PNJ length and a sharp decrease in the peak intensity. The use of a single-layer array of identical microtoroids changes the structure of the near-field scattering. The impact of neighbouring particles in the PNJ formation is associated with mutual interference of optical fields and is manifested mainly in pulsations of the PNJ intensity and length, which leads to a spatial 'break' of the PNJ into separate segments along the direction of optical wave propagation when the cluster lattice period changes. This effect is most pronounced for densely packed particles.

It is shown that with a certain arrangement of particles in the cluster, it becomes possible to implement PNJs with parameters significantly better than those for an isolated toroid. Thus, the diffraction interaction of fields from individual toroids can significantly increase the overall length of the jet (in the case of densely packed particles). Moreover, the use of particle clusters almost always, with the exception of certain cases, leads to the formation of PNJs with higher peak intensities, which is a fundamental point in solving a number of practical problems.

Acknowledgements. This work was performed within the framework of the State Assignment of Zuev Institute of Atmospheric Optics, Siberian Branch of the Russian Academy of Sciences, as well as was partially supported by the Russian Foundation for Basic Research (Grant No. 19-47-700001).

References

1. Allen K.W., Farahi N., Astratov V.N., Li Y. *Annal. Phys.*, **527** (7-8), 513 (2015).
2. Wu W., Katsnelson A., Memis O.G., Mohseni H. *Nanotechnol.*, **18**, 485302 (2007).
3. Chen Z., Taflove A., Backman V. *Opt. Express*, **12** (7), 1214 (2004).
4. Li X., Chen Z., Taflove A., Backman V. *Opt. Express*, **13** (2), 526 (2005).
5. Geints Yu.E., Panina E.K., Zemlyanov A.A. *Opt. Atmos. Okeana*, **25** (5), 417 (2012).
6. Heifetz A., Huang K., Sahakian A.V., Li X., Taflove A., Backman V. *Appl. Phys. Lett.*, **89**, 221118 (2006).
7. Geints Yu.E., Panina E.K., Zemlyanov A.A. *J. Opt. Soc. Am. B*, **28**, 1825 (2011).
8. Geints Yu.E., Panina E.K., Zemlyanov A.A. *J. Quant. Spectrosc. Radiat. Transfer*, **126**, 44 (2013).
9. Itagi A.V., Challener W.A. *J. Opt. Soc. Am. A*, **22** (12), 2847 (2005).
10. Geints Yu.E., Panina E.K., Zemlyanov A.A. *Opt. Atmos. Okeana*, **31** (9), 706 (2018).
11. Minin I.V., Minin O.V., Geints Yu.E. *Ann. Phys. (Berlin)*, **527**, 491 (2015).
12. Minin I.V., Minin O.V., Pacheco-Pena V., Beruete M. *Opt. Lett.*, **40**, 2329 (2015).
13. Kato S., Chonan S., Aoki T. *Opt. Lett.*, **39**, 773 (2014).
14. Chang C.-H. *Nano Lett.*, **11** (6), 2533 (2011).
15. Zhu J., Goddard L.L. *Nanoscale Adv.*, **1**, 4615 (2019).
16. Chen L., Zhou Y., Li Y., Hong M. *Appl. Phys. Rev.*, **6**, 021304 (2019); https://doi.org/10.1063/1.5082215.
17. Pacheco-Peña V., Beruete M. *J. Appl. Phys.*, **125**, 084104 (2019); https://doi.org/10.1063/1.5086175.
18. Sergeeva K.A., Tutov M.V., Voznesenskiy S.S., Shamich N.I., Mironenko A.Yu., Sergeev A.A. *Sensors Actuators B: Chemical*, **305**, 127354 (2020).
19. Bityurin N., Afanasiev A., Bredikhin V., Alexandrov A., Agareva N., Pikulin A., Ilyakov I., Shishkin B., Akhmedzhanov R. *Opt. Express*, **21**, 21485 (2013).
20. Gentselev A.N., Gol'denberg B.G., Kondrat'ev V.I., Petrova E.V. Russian Federation Patent No. 2350996 (2009).
21. Lebedev-Stepanov P.V., Kadushnikov R.M., Molchanov S.P., Ivanov A.A., Mitrokhin V.P., Vlasov K.O., Rubin N.I., Yurasik G.A., Nazarov V.G., Alfimov M.V. *Ross. Nanotekhnol.*, **8** (3-4), 5 (2013).
22. Chan C.-H., Fischer A., Martinez-Gil A., Taillepierre P., Lee C.-C., Yang S.-L., Hou C.-H., Chien H.-T., Cai D.-P., Hsu K.-C. *Appl. Phys. B*, **100**, 547 (2010).
23. Brétagnol F., Ceriotti L., Valsesia A., Sasaki T., Ceccone G., Gilliland G., Colpoand P., Ross F. *Nanotechnol.*, **18**, 135303 (2007).

24. Rizzato S., Primiceri E., Monteduro A.G., Colombelli A., Leo A., Manera M.G., Rella R., Maruccio G. *Beilstein J. Nanotechnol.*, **9**, 1582 (2018).
25. Wang Z.B., Guo W., Luk'yanchuk B., Whitehead D.J., Li L., Liu Z. *J. Laser Micro/Nanoeng.*, **3** (1), 14 (2008).
26. Geints Yu.E., Panina E.K., Zemlyanov A.A. *Opt. Atmos. Okeana*, **32** (2), 113 (2019).
27. Geints Yu.E., Zemlyanov A.A., Panina E.K. *Quantum Electron.*, **49** (3), 210 (2019) [*Kvantovaya Elektron.*, **49** (3), 210 (2019)].
28. Geints Yu.E., Zemlyanov A.A., Panina E.K. *Quantum Electron.*, **46** (3), 236 (2016) [*Kvantovaya Elektron*., **46** (3), 236 (2016)].
29. Zhang B., Hao J., Shen Z., Wu H., Zhu K., Xu J., Ding J. *Appl. Opt.*, **57** (28), 8331 (2018).
30. Golovashkin D.L., Doskolovich L.L., Kazanskii N.L. *Difraktsionnaya komp'yuternaya optika* (Diffraction Computer Optics) (Moscow: Fizmatlit, 2007).
31. Geints Yu.E., Zemlyanov A.A., Panina E.K. *Quantum Electron.*, **41** (6), 520 (2011) [*Kvantovaya Elektron.*, **41** (6), 520 (2011)].